

Airborne thermal remote sensing for water temperature assessment in rivers and streams

Christian E. Torgersen^{a,*}, Russell N. Faux^b, Bruce A. McIntosh^{b,1}, Nathan J. Poage^b,
Douglas J. Norton^c

^a*Oregon Cooperative Fish and Wildlife Research Unit, Department of Fisheries and Wildlife, Oregon State University, 104 Nash Hall, Corvallis, OR 97331, USA*

^b*Forestry Sciences Laboratory, Department of Forest Science, Oregon State University, Corvallis, OR, USA*

^c*Office of Water, U.S. Environmental Protection Agency, Washington, DC, USA*

Received 19 July 2000; accepted 29 December 2000

Abstract

Airborne remote sensing methods are needed to assess spatial patterns of stream temperature at scales relevant to issues in water quality and fisheries management. In this study, we developed an airborne remote sensing method to measure spatially continuous patterns of stream temperature and evaluated the physical factors that influence the accuracy of thermal remote sensing of flowing waters. The airborne thermal infrared (TIR) system incorporated an internally calibrated thermal imager (8–12 μm) aligned with a visible band camera in a vertically mounted, gimbaled pod attached to the underside of a helicopter. High-resolution imagery (0.2–0.4 m) covering the entire channel and adjacent floodplains was recorded digitally and georeferenced in-flight along 50- to 60-km river sections ranging from 2 to 110 m in width. Radiant water temperature corresponded to kinetic water temperature (5–27°C) in a range of stream environments within $\pm 0.5^\circ\text{C}$. Longitudinal profiles of radiant water temperature from downstream to headwater reaches provided a spatial context for assessing large-scale patterns of thermal heterogeneity and fine-scale thermal features such as tributaries and groundwater inputs. Potential sources of error in remote measurements of stream temperature included reflected longwave radiation, thermal boundary layer effects at the water surface, and vertical thermal stratification. After taking into account the radiative properties of the surrounding environment and the physical qualities of the stream, thermal remote sensing proved highly effective for examining spatial patterns of stream temperature at a resolution and extent previously unattainable through conventional methods of stream temperature measurement using in-stream data recorders. © 2001 Elsevier Science Inc. All rights reserved.

1. Introduction

Water temperature in rivers and streams has been identified as a critical element in the restoration of freshwater aquatic ecosystems and the recovery of salmon in the Pacific Northwest region of the United States (McCullough, 1997; Naiman, Magnuson, McKnight, Stanford, & Karr, 1995; Nehlsen, Williams, & Lichatowich, 1991; NRC, 1992). As an index of water quality, stream temperature reflects watershed and stream corridor conditions and directly influences the biology of aquatic organisms

(Beschta, Bilby, Brown, Holtby, & Hofstra, 1987). To promote improvements in water quality and protect threatened and endangered aquatic biota, Section 303d of the Clean Water Act (United States Congress, 1977) requires states and the U.S. Environmental Protection Agency to maintain a list of stream segments that do not meet water quality standards. In response to Federal requirements, some states have established specific stream temperature standards to identify rivers and streams in which water temperature exceeds the thermal tolerances of native species of salmon and trout (Boyd & Sturdevant, 1997). Stream temperature monitoring presents challenges for water resource managers charged with the task of administering many kilometers of streams that flow through public and private lands. Conventional methods of stream temperature measurement using in-stream data recorders provide information that is temporally continuous but spatially limited.

* Corresponding author. Tel.: +1-541-737-2463; fax: +1-541-737-3590.

E-mail address: ctorgersen@orst.edu (C.E. Torgersen).

¹ Current address: Corvallis Research Laboratory, Oregon Department of Fish and Wildlife, Corvallis, OR, USA.

Spatial data are needed to map sources of thermal heterogeneity at the watershed scale and identify biologically important areas such as thermal refugia (Torgersen, Price, Li, & McIntosh, 1999).

Remote sensing methods for monitoring stream temperature can alleviate problems of access to private lands and provide a spatial context for evaluating relationships between land use and water quality. Stream temperature patterns are influenced by multiple land-use practices that remove riparian vegetation and alter channel morphology and streamflow (Holtby, 1988; Johnson & Jones, 2000; LeBlanc, Brown, & FitzGibbon, 1997). The response of stream temperature to landscape change is difficult to predict, and as a consequence, considerable debate exists about the relative influence of various land management practices on stream temperature (Beschta, 1997; Larson & Larson, 1996; Zwieniecki & Newton, 1999). However, integration of spatial data in stream temperature models will be useful for validating models and understanding the effects of land management practices on stream temperature (Chen, Carsel, McCutcheon, & Nutter, 1998; Chen, McCutcheon, Norton, & Nutter, 1998; Norton et al., 1996).

Applications of TIR remote sensing have been important in obtaining sea surface temperature measurements for oceanographic and meteorological applications (Jessup, Zappa, Loewen, & Hesany, 1997; Smith, Knuteson, & Revercomb, 1996). In addition, freshwater applications of TIR remote sensing have been conducted to map surface temperature and circulation patterns in lakes (Anderson, Duck, & McManus, 1995; Garrett & Hayes, 1997; Lathrop & Lillesand, 1987; LeDrew & Franklin, 1985), model heat dispersion in thermal effluent plumes (Davies, Mofor, & Neves, 1997; Jensen, Ramsey, Mackey, & Hodgson, 1988; Schott, 1979), and identify subsurface springs (Roxburgh, 1985). However, few studies have been conducted with the explicit purpose of mapping patterns of water temperature in riverine environments because concerns about elevated stream temperatures and the implications for coldwater fishes have only recently been raised (Atwell, McDonald, & Bartolucci, 1971; Belknap & Naiman, 1998; Torgersen et al., 1999).

Airborne thermal infrared (TIR) remote sensing has potential for addressing current needs in water resources science for spatial assessment and monitoring of stream temperature. The application of remote temperature measurement in rivers and streams is a relatively recent development and has proven effective for assessing stream temperature patterns in relation to habitat use by salmon (Belknap & Naiman, 1998; Torgersen et al., 1999). However, in spite of the applicability of remote sensing technology to stream temperature measurement there has been no comprehensive description of either a method or the physical factors that influence remote sensing of flowing waters since the development of airborne digital thermal imagers (Atwell et al., 1971). In this study, our objectives were to: (1) develop an airborne thermal remote sensing method to

measure spatially continuous patterns of water temperature in rivers and streams, (2) assess the temperature accuracy of aerial thermography in varied riverine environments and identify the sources of error in thermal imagery of flowing waters, and (3) evaluate the potential of airborne thermal remote sensing for assessing spatial heterogeneity in stream temperature at multiple scales ranging from high-resolution imagery of tributary confluences and groundwater inputs (0.2–0.4 m) to longitudinal profiles of entire river sections (50–60 km).

2. Methods

2.1. Thermal remote sensing of water temperature

Remote measurements of water temperature are made with a sensor that detects thermal radiation (3–5 and 8–14 μm wavebands) emitted from the upper 0.1 mm of the water surface (Anderson & Wilson, 1984; Atwell et al., 1971; Robinson, Wells, & Charnock, 1984). We define the temperature of the water surface measured remotely with a thermal sensor as the radiant water temperature (T_r) as opposed to the kinetic water temperature (T_k) measured 10 cm below the surface with a thermometer. Radiant water temperature measurements are representative of T_k when the water column is sufficiently mixed and thermal gradients have not formed as a function of depth.

The factors that influence measurements of T_r are emissivity, atmospheric absorption, TIR reflection, and surface characteristics (Smith et al., 1996). Emissivity describes the actual absorption and emission properties of the water surface and is expressed as a ratio of the emittance from the water surface at a given temperature to that from a black body at the same temperature (Avery & Berlin, 1992). Because water has an emissivity very close to 1.0 and a high thermal inertia, it is relatively easy to obtain measurements of T_r compared to land surfaces. Atmospheric effects can be corrected based on water vapor content and transmission along the target sensor path, but TIR reflections can complicate precise temperature measurement because a thermal sensor measures longwave radiation that is both emitted and reflected from the water surface (Anderson & Wilson, 1984; Schott, 1994). Thus, emitted radiation transmits temperature information from the water surface itself as well as reflected radiation from the surrounding environment (Fig. 1).

2.2. Airborne TIR system

Thermal imagery in the 8–12 μm waveband was collected with a Thermovision 1000 forward-looking infrared (FLIR) system (FLIR Systems). The scanning array thermal imager used built-in blackbody temperature references to continuously calibrate the HgCdTe multi-element detectors. The FLIR thermal imaging system incorporated 12-bit

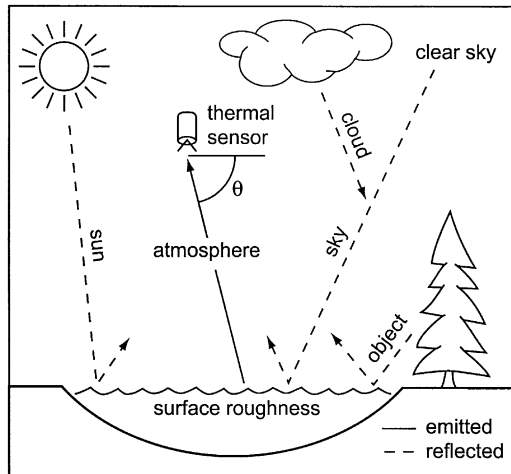


Fig. 1. Sources of emitted and reflected TIR radiation in thermal remote sensing of rivers and streams.

signal processing and was capable of detecting noise-equivalent temperature differences of $\pm 0.2^\circ\text{C}$.

Visible spectral band imagery ($0.4\text{--}0.7\ \mu\text{m}$) was collected with a VX-1000 digital video camera (Sony Electronics) with a 3-chip charge-coupled device (CCD) imaging system. Thermal and visible cameras covered the same ground area with a $20 \times 13^\circ$ field-of-view and an image size of 600×400 pixels. The two sensors were aligned for vertical view in a gyro-stabilized, gimballed pod attached to the underside of a Bell 206B-3 helicopter. Thermal images were collected digitally and recorded directly from the sensor to an on-board computer at a rate of 1 frame/s. At this rate, the FLIR system stored digital imagery at a rate of 2.5 gigabytes/h. Digital image files represented the full 12-bit dynamic range of the sensor and were tagged with acquisition time and differentially corrected geographic position data provided by a Trimble aeronautical global positioning system (GPS). Visible band imagery and acquisition time were recorded to an on-board digital video recorder at a rate of 30 frames/s. Downlinks of Greenwich Mean Time (GMT) from the GPS synchronized data collection to the nearest second and provided a means of correlating thermal and visible band imagery during postflight image processing.

2.3. TIR data collection

The objective of aerial thermography was to examine patterns of T_r during summer low streamflow conditions. We conducted thermal overflights on cloudless days in late July through early September that at times coincided with maximum daily stream temperatures. Peak daily stream temperatures occurred at 14:00–18:00 in the afternoon, approximately halfway between land–water thermal cross-over periods (Fagerlund, Kleman, Sellin, & Svensson, 1970). Meteorological data on air temperature, relative humidity, cloud cover, and surface winds were collected at

local airports before, during, and after overflights and from U.S. National Weather Service remote automated weather stations distributed throughout the survey area.

Airborne thermal remote sensing at low altitudes required coordination between the helicopter pilot, navigator, and FLIR operator. Real-time GPS positioning and flight plan software provided map information necessary for locating start and end points of stream survey sections. Fine-scale adjustments of the flight path and altitude were made visually by the pilot in cooperation with the FLIR operator and navigator. Aerial surveys were conducted in an upstream direction. Flight altitude and speed varied depending on stream width, sinuosity, and valley configuration. Low-altitude aerial surveys along the streams required constant compensation for land surface elevation change as a function of stream gradient. Radar altimetry was essential for maintaining, adjusting, and recording sensor height above ground level (AGL). Typical flight altitudes of 300–700 m AGL provided imagery with ground resolutions of 0.2–0.4 m sufficient for measuring T_r in streams and side channels 2–110 m in width. Ground speeds were maintained at 50 km/h over narrow, sinuous streams and increased to 90 km/h over wide, straight rivers. Speeds in this range ensured approximately 40–60% overlap between image frames stored at a rate of 1 frame/s. To avoid image blur in the CCD digital video imagery, the speed of the aircraft was reduced at very low sensor heights.

Images from the thermal sensor were stored digitally with each pixel containing the radiance value measured by the detector. Thermal radiance values were converted to temperatures using Planck's radiation law and sensor calibration curves (Atwell et al., 1971). Radiant water temperatures were adjusted for the emissivity of natural water (0.96) and corrected for atmospheric transmissivity and ambient reflections using the LOWTRAN-7 atmospheric simulation model with inputs of air temperature, relative humidity, and path length (Kneizys et al., 1988; Schott, 1994). The converted images were ultimately stored in a format in which each pixel contained a temperature value rounded to the nearest 0.1°C . Thermal imagery was color-coded to visually enhance temperature differences and facilitate interpretation of thermal patterns.

2.4. Study areas and field measurements

Field data used in this study were collected in watersheds representing a wide range of riverine environments in western and eastern Oregon ($44\text{--}46^\circ\text{N}$, $117\text{--}123^\circ\text{W}$). Rivers and streams selected for thermal survey included the upper McKenzie River (western Oregon), the Middle and North forks of the John Day River, the North Fork of the Malheur River, and the Wenaha River (all in eastern Oregon). We surveyed moderate- to fast-flowing mountain streams ($0.3\text{--}1.1\ \text{m/s}$ average velocity) in canyons and alluvial valleys that ranged in elevation from 300 to 2000 m and had gradients of 0.4–2.0% (Table 1). Surveyed

Table 1
Physical characteristics of streams surveyed with airborne thermal remote sensing

Stream	Section characteristics				Channel characteristics		
	Valley type ^a	Length (km)	Elevation (m)	Gradient (%)	Channel type ^b	Width (m)	Depth (m)
McKenzie River	cc, ac	45	300–650	0.8	s, m	15–110	0.2–6.0
Middle Fork John Day River	ac, av	70	1000–1300	0.4	s, m, a	3–15	0.1–3.0
North Fork John Day River	cc, ac	70	850–1750	1.3	s, m	5–30	0.2–4.0
North Fork Malheur River	cc, av	55	1000–2000	2.0	s, m	2–10	0.1–2.0
Wenaha River	cc, ac	45	500–850	0.8	s, m, b	4–30	0.2–4.0

^a Valley types in survey streams included colluvial canyons (cc), alluviated canyons (ac), and alluvial valleys (av) (Frissell, 1992).

^b Channel types observed are classified as straight (s), meandering (m), braided (b), or anastomosing (a) after Selby (1985).

stream sections contained straight, meandering, braided, and anastomosing channel types that averaged ≈ 0.5 m in depth in all streams except for the McKenzie River, which was significantly wider and deeper than all other streams (Table 1). Canopy cover from conifer and broadleaf riparian vegetation ranged from completely closed (i.e., no measurements of T_r could be made) to wide open and was variable in extent and composition within and among the streams surveyed. Differences in regional climate, relative humidity (15–30%), and canopy cover type and extent among streams provided varied environments in which to assess the effectiveness of airborne TIR remote sensing for stream temperature assessment.

Ground-truth measurements were collected simultaneously with thermal overflights to compare T_k to T_r recorded in the imagery. Ground-truth measurements of T_k were made with submersible digital temperature recorders (Onset, accuracy $\pm 0.2^\circ\text{C}$) programmed to sample T_k once every minute and positioned in the well-mixed portion of the stream water column. Postflight measurements of thermal stratification were collected in deep pools and spring-fed side channels 10 cm below the surface and 10 cm above the stream bottom with calibrated digital thermometers (Atkins) and an immersible, stainless steel thermocouple (VWR Scientific) accurate to $\pm 0.1^\circ\text{C}$.

To evaluate variations in T_k as a function of water depth, thermal stratification measurements were collected during the following year under similar seasonal and diurnal conditions as thermal overflights. We identified areas of potential thermal stratification in the thermal imagery and measured surface and bottom T_k in $\times 1$ m grids across the water surface at a total of five sites in the Middle Fork John Day River, Granite Creek (a tributary of the North Fork John Day River), and the Wenaha River. To assess the temporal dynamics of thermal stratification, we sampled thermal transects in the morning and afternoon on several different dates under both clear and cloudy weather conditions.

2.5. TIR data analysis

Point pattern maps of thermal surveys were constructed in a geographical information system (GIS) to provide a template for sampling and displaying longitudinal T_r pat-

terns in each stream section. A computer program was used to scan sequential thermal image files and extract time and geographic coordinate information to create a map of image collection points. Thermal and visible image pairs were linked to points and sampled directly within the GIS environment. In producing spatially continuous profiles of T_r thermal image frames were analyzed individually as opposed to image composites or mosaics. Values of T_r were sampled manually from each thermal image in the main stream channel at 10 points in each image. Sample points were selected in each image by evaluating fluvial characteristics to identify areas of main stream flow and avoid partially submerged rocks and large woody debris. Sample median of T_r (T_{rs}) for each image was automatically calculated from the 10 sample points and updated in the GIS spatial database. Digital hydrography data (1:100,000 scale) provided the map template for longitudinal analysis of T_{rs} patterns in the study streams. The route-measure or river km system was employed to record the locations of thermal image collection points along the longitudinal stream profile. Route-measure coordinates of image collection points were expressed as cumulative distance upstream from the river mouth.

Analysis of thermal image sequences at multiple spatial scales required the integration of longitudinal profiles of T_{rs} , maps of image collection points, and individual image frames. Coarse-scale sources of thermal heterogeneity were identified in longitudinal profiles and located on point pattern maps of aerial surveys. Individual image points were then queried to visually inspect thermal imagery and locate sources of cold- or warm-water inputs. Fine-scale temperature patterns in thermal image frames were examined and compared with hydrologic features and channel morphology in visible spectral band imagery.

Values of T_{rs} were compared with ground-truth measurements to assess the relationship between airborne TIR measurements and T_k . We calculated the average absolute difference and standard error (S.E.) between measurements of T_k and T_{rs} collected during each overflight for four survey years. Linear regression was used to assess the statistical relationship between T_k and T_{rs} . To examine the relationship between the frequency distribution of temperature pixels within the stream channel and ground-truth measurements, we computed histograms of pixel frequency

versus T_r in streams of different width and compared population median radiant water temperature (T_{rp}) and T_{rs} to measurements of T_k .

We assessed thermal stratification and its potential for introducing error in remote sensing of water temperature by comparing bottom and surface T_k at five sites during the years following thermal overflights. Bottom–surface temperature differences were calculated for each 1×1 -m sampling grid. Thermal stratification was then estimated by comparing the proportion of temperature differences $\geq 0.2^\circ\text{C}$ among sites under different environmental conditions. Plots depicting the spatial distribution of bottom–surface temperature differences were constructed to compare the patterns of T_k with thermal imagery collected the previous year.

3. Results

3.1. Spatial patterns of radiant water temperature

Profiles of T_{rs} versus distance upstream provided a spatially continuous representation of longitudinal patterns in stream temperature in the McKenzie River and the Middle Fork John Day River (Fig. 2). Tributary confluence T_{rs} plotted where the tributaries enter the main stream channel indicated where and to what extent surface water

inputs influence mainstem temperature. For example, Ollalie Creek, which has high volumetric flow relative to the main stream channel, caused decreases of $1\text{--}2^\circ\text{C}$ in mainstem temperature where it entered the McKenzie River (Fig. 2A). Values of T_{rs} from the thermal imagery corresponded well to ground-truth measurements of T_k over the wide range of temperatures in both study streams.

Remotely sensed thermal profiles in the study streams revealed patterns of spatial variability in T_{rs} and provided a means of characterizing the thermal signature of individual streams or rivers. The temperature of the Middle Fork John Day River increased 3.5°C over 50 km and displayed a dramatic series of peaks and troughs in a downstream direction (Fig. 2B). In contrast to the Middle Fork, McKenzie River temperatures increased rapidly (5.0°C) over a similar distance and were much more homogeneous (Fig. 2A). Peaks and troughs in temperature that occurred over short distances in the longitudinal stream profile typically indicated tributary inputs (Fig. 2A; Ollalie Creek), whereas large-scale patterns, such as gradual warming trends and large troughs covering 5–10 km, reflected physical geomorphic, riparian, and hydrologic processes occurring at the watershed scale (Fig. 2B).

Longitudinal profiles of T_{rs} provided a watershed context for analyzing thermal patterns and hydrologic features depicted in individual thermal and visible band images. High spatial resolution imagery of the stream channel was useful for identifying and evaluating the influence of thermal inputs to the main stream channel such as tributaries (Fig. 3A) and groundwater–surface water exchange in (Fig. 3B). Visible band imagery facilitated differentiation between land and water surfaces in thermal images and classification of hydrologic features and channel morphology. Mosaics of thermal and visible band imagery were useful for qualitative assessment and presentation purposes but not for quantitative analysis because the imagery was not photogrammetrically rectified.

3.2. Temperature accuracy of TIR remote sensing

Values of T_{rs} were consistently within $\pm 0.5^\circ\text{C}$ of ground-truth measurements of T_k over four survey years in five different streams (Table 2). The average absolute temperature difference between T_{rs} and T_k for all four survey years was 0.3°C . Of the five streams surveyed, the streams with the narrowest stream channels (Middle Fork John Day River and North Fork Malheur River) had the greatest average absolute temperature differences (Tables 1 and 2). For all years and streams combined, T_{rs} measurements predicted T_k in a near perfect 1:1 relationship ($r^2=0.99$) with slightly increased error occurring at warmer temperatures (Fig. 4).

Histograms of pixels in the stream channel provided information on the distribution of T_r in the thermal imagery (Fig. 5). Values of T_{rs} were generally within $\pm 0.5^\circ\text{C}$ of T_{rp} and T_k , and T_{rs} was equivalent to T_{rp} when the distribution of T_r was not skewed (Fig. 5A and C). However, when the

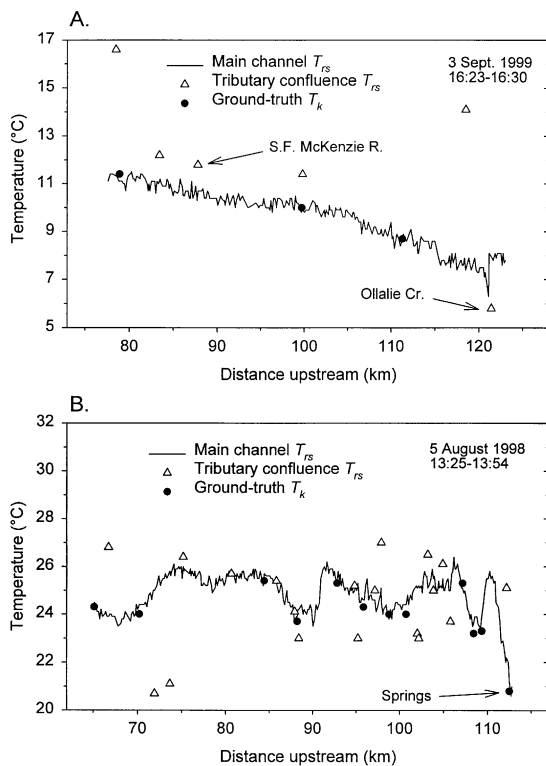


Fig. 2. Longitudinal profiles of sample median radiant water temperature (T_{rs}) and ground-truth measurements of kinetic water temperature (T_k) in the McKenzie River (A) and the Middle Fork John Day River (B). Measurements of tributary confluence T_{rs} are plotted where the tributaries enter the main stream channel.

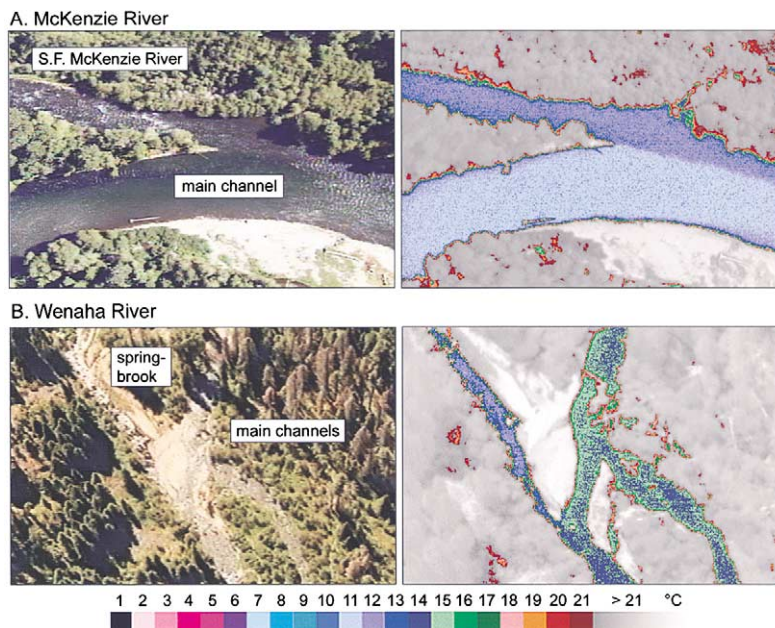


Fig. 3. Hydrologic features and channel morphology in paired TIR and visible band images of the McKenzie River (A) and the Wenaha River (B). Colors in the thermal images represent radiant water temperature (T_r) in $^{\circ}\text{C}$. Image frames for the McKenzie River and the Wenaha River represent ground areas of 216×144 and 261×174 m, respectively.

distribution of T_r in the stream channel was slightly or severely skewed (Fig. 5B and D, respectively), T_{rs} provided a more accurate estimate of T_k than T_{rp} . The primary cause for skewness in histograms of T_r was narrow stream width (i.e., <9 pixels). Values of T_{rp} in the narrowest stream were skewed towards higher temperatures as indicated by a difference of 0.8°C between T_{rp} and T_k (Fig. 5D). When the stream was narrow relative to the ground cell resolution, relatively few pixels in the stream channel contained only

water surfaces. Thus, T_{rp} in narrow streams was skewed towards higher temperatures due to the large proportion of hybrid pixels that encompassed both land and water surfaces at the stream margins. In addition to land–water averaging in narrow streams, skewness in T_{rp} towards higher values also occurred in wide streams where the characteristics of the water surface changed from smooth to rough within a single image frame (Fig. 5B).

3.3. Thermal stratification measurements

Study sites in the Middle Fork John Day River, Granite Creek (North Fork John Day River), and Wenaha River varied widely in physical characteristics and provided a setting for in situ evaluation of thermal stratification in

Table 2

Average absolute temperature differences between sample median radiant water temperature (T_{rs}) and ground-truth measurements of kinetic water temperature (T_k)

Stream and year ^a	Number of ground-truth points	Average absolute temperature difference ($^{\circ}\text{C}$) ^b	S.E.
McKenzie River			
1999	6	0.20	0.05
Middle Fork John Day River			
1994	9	0.4	0.1
1996	13	0.5	0.1
1998	14	0.30	0.05
North Fork John Day River			
1994	4	0.30	0.05
1998	8	0.20	0.05
North Fork Malheur River			
1998	3	0.40	0.03
Wenaha River			
1998	10	0.30	0.05

^a Aerial thermal surveys conducted before 1998 used different FLIR systems described by Poage et al. (1996) and Torgersen et al. (1999).

^b Average absolute temperature differences were calculated from comparisons between T_{rs} and T_k collected during thermal overflights at specific points along the spatial extent of the survey reach.

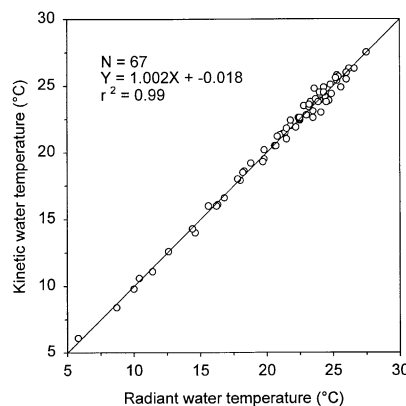


Fig. 4. Linear regression analysis of ground-truth kinetic water temperature (T_k) versus sample median radiant water temperature (T_{rs}) for four survey years in five different streams (see Table 2).

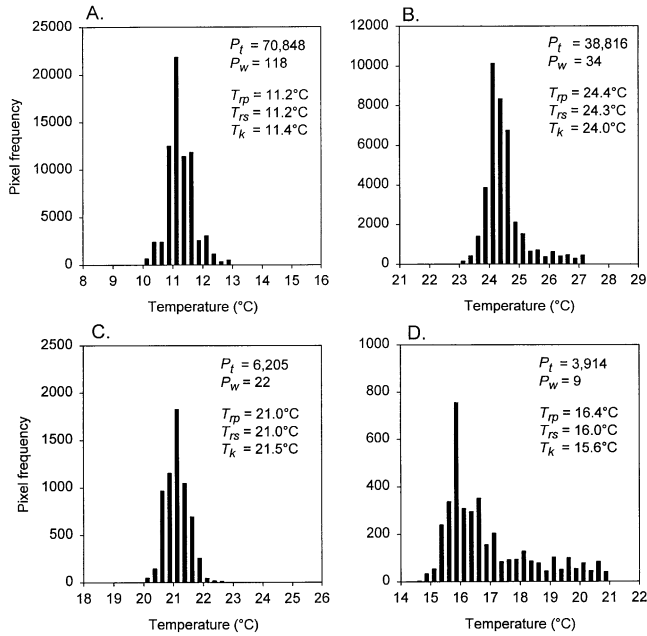


Fig. 5. Histograms of radiant water temperature (T_r) in images of stream channels in the McKenzie River (A), the Middle Fork John Day River (B), and the North Fork Malheur River (C and D). Statistics for each histogram include total number of pixels (P_t), stream width measured in pixels (P_w), population median radiant water temperature (T_{tp}), sample median radiant water temperature (T_{ts}), and kinetic water temperature (T_k).

main- and side-channel stream environments (Table 3A). Study site GC4 in Granite Creek contained the deepest pool with a maximum depth of 3.20 m, and study site WEN1, a spring-fed alcove in the Wenaha River, had the second deepest pool at 1.31 m. Temperature differences in the water column were considered significant if bottom–surface

temperature differences exceeded the $\pm 0.1^{\circ}\text{C}$ accuracy of the digital thermometer with which T_k measurements were made. Granite Creek (GC4) and WEN1 were the only sites that exhibited thermal stratification (Table 3B). Thermal stratification was most pronounced during clear/sunny conditions when solar heating at the water surface occurred faster than vertical mixing caused by stream flow. Under these environmental conditions, surface T_k was warmer than bottom T_k unless turbulent mixing brought cold water to the surface. Temperature measurements in WEN1 were collected only under clear/sunny conditions because cold groundwater inputs and limited vertical mixing at this site resulted in a constant stratified thermal profile during all weather conditions.

Thermal stratification in GC4 and WEN1 was minimal, even under environmental conditions in which we expected to find pronounced stratification (Fig. 6). Comparisons of bottom and surface T_k in the deep pool in GC4 revealed only minimal stratification, and surface T_k patterns reflected cooler subsurface temperatures towards the deepest section of the pool (Fig. 6A and B). Thermal stratification in WEN1, the groundwater-influenced site, was more pronounced than in GC4 (Fig. 6D). The degree of stratification in this site increased with depth along the longitudinal transect to $\approx 1^{\circ}\text{C}$. Surface T_k in WEN1 also increased along the longitudinal transect from the spring outflows to the main river channel (Fig. 6C).

Patterns of T_r sampled from imagery corresponded with surface T_k measurements collected during the following year. Absolute values of T_r and T_k were different because daily maximum air temperature differed between years. However, the relative spatial patterns of T_r and T_k were similar because the physical characteristics and hydrologic

Table 3

(A) Physical characteristics of thermal stratification study sites in the Middle Fork John Day River (MFJD), Granite Creek (GC4), and the Wenaha River (WEN1)

Study site	Length (m)	Width (m)	Maximum depth (m)	Mean depth (m)	Channel type ^a	Number of sample points
MFJD1	33	9	1.11	0.43	PR	40
MFJD2	31	11	0.93	0.38	PR	50
MFJD3	28	8	0.86	0.36	PR	32
GC4	28	25	3.20	1.24	PO	89
WEN1	50	3	1.31	0.64	PO	18

(B) Proportions of bottom–surface kinetic water temperature (T_k) differences (Δ) in thermal stratification study sites under different meteorological conditions

Study site	Clear/sunny conditions			Cloudy/rainy conditions			
	N^b	Δ Temperature ($^{\circ}\text{C}$)		N	Δ Temperature ($^{\circ}\text{C}$)		
		0 ± 0.1	≥ 0.2		0 ± 0.1	≥ 0.2	≤ -0.2
MFJD1	129	1.00	–	73	1.00	–	–
MFJD2	177	0.98	0.01	92	1.00	–	–
MFJD3	120	0.98	0.01	61	0.98	–	0.02
GC4	243	0.93	0.00	126	1.00	–	–
WEN1	18	0.61	0.10	NA	NA	NA	NA

^a Pool-riffle study sites (PR) contained one pool bounded by two riffles. Pool study sites (PO) contained one large pool.

^b Total number of bottom–surface comparisons in each site. The degree of thermal stratification is represented by the proportion of comparisons within a specified temperature range.

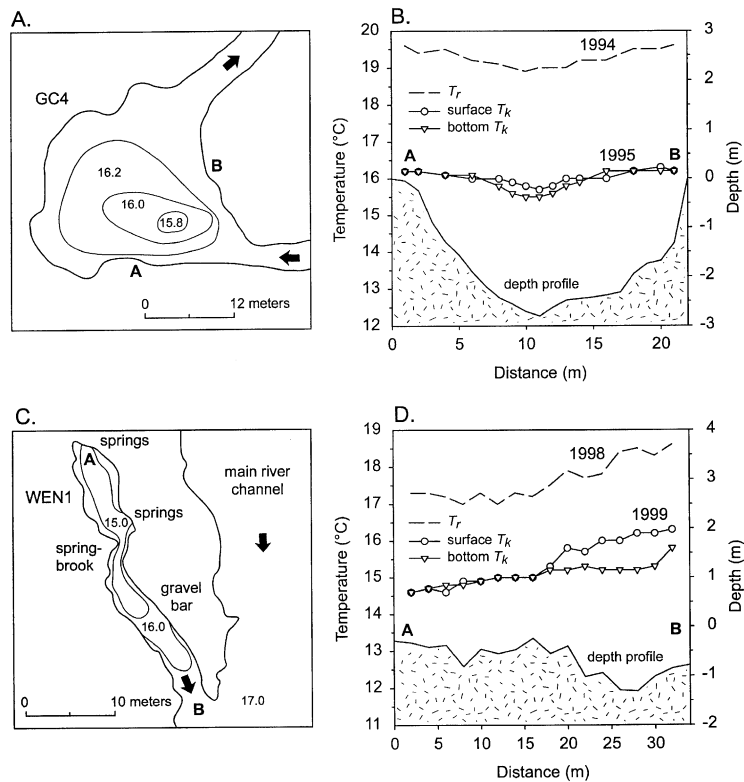


Fig. 6. Spatial patterns of radiant and kinetic water temperatures (T_r and T_k , respectively) and depth in thermally stratified pools in study sites GC4 in Granite Creek (A and B) and WEN1 in the Wenaha River (C and D). Kinetic water temperatures ($^{\circ}\text{C}$) and the location of thermal transects A and B are plotted on schematics of each pool (A and C). Thermal stratification measurements of T_k were collected during the year following remote sensing overflights in order to compare spatial patterns (not absolute values) of T_k and T_r .

properties of the two pools had not changed noticeably since the thermal overflight. Patterns of T_r in GC4 paralleled T_k such that both T_k and T_r were slightly cooler towards the center of the pool (Fig. 6B). In WEN1, the spring-fed alcove, patterns in T_r matched both the trend and the magnitude of T_k measurements collected during the following year (Fig. 6D).

4. Discussion

4.1. Airborne TIR remote sensing system

Remote sensing of water temperature in rivers and streams is an exclusively airborne application that requires high-resolution imagery for mapping thermal patterns in streams with widths as narrow as 2 m. Sensor height is determined by stream width as opposed to stream length, and temperature measurement requires a linear survey method fundamentally different from remote sensing conducted from high-altitude platforms. Airborne remote sensing of streams shares methodological similarities with transect approaches such as airborne laser altimetry (Ritchie, Grissinger, Murphey, & Garbrecht, 1994; Ritchie et al., 1993). However, surveys of a stream or river surface must follow a sinuous path, as opposed to a straight line, and

simultaneously adjust for changes in ground elevation as a function of stream gradient. The specific requirements of thermal remote sensing of streams necessitate the use of helicopter rather than fixed-wing platforms in thermal surveys. Helicopters are costly to operate and have a restricted altitudinal and horizontal operating range, but they enable sensor height adjustments over short ground distances and thereby ensure maximum pixel coverage within the stream channel necessary for water temperature measurement. Analysis of pixel frequency distributions in thermal imagery of narrow stream channels indicates that temperature accuracy is compromised at stream widths less than 10 pixels (Fig. 5D). Thus, it is necessary to maintain a sensor height low enough for resolving the stream surface in as many pixels as possible. In thermal surveys of small streams, in-flight estimations of stream width in pixels provide the pilot with a visual, scaled reference on which to base altitude adjustments.

The TIR system for measuring T_r requires specialized data collection, preparation, and sampling procedures in order to provide stream temperature data in a format that is accessible and usable in water resources applications. Internally calibrated thermal imagers measure stream temperature accurately and facilitate immediate analysis with minimal postflight calibration requirements. Sensors that measure thermal radiance in either longwave or midwave

thermal regions (8–12 and 3–5 μm , respectively) both provide adequate measurements of T_r (Anderson & Wilson, 1984). However, the bulk of emitted radiation from natural water bodies (0–30°C) is in the longwave region of the spectrum, and longwave systems are less sensitive to solar reflections than systems operating in the midwave region. Midwave systems can be filtered to reduce solar reflections and are typically more sensitive radiometrically than longwave systems, but for in situ measurements of T_r where environmental factors alone account for errors of $\pm 0.5^\circ\text{C}$, the added sensitivity of midwave systems may be unnecessary.

Thermal image collection and processing is an important practical consideration in thermal remote sensing of streams. Image acquisition in digital format directly from the sensor is recommended over video recording. Thermal imagery can be recorded to SVHS videotape, digitized, and processed postflight to extract pixel values if sensor settings are locked in a specific temperature range (e.g., 5–55°C) and displayed as 8-bit images with 256 gray-levels (Poage, Torgersen, Norton, & Flood, 1996). Video recording of imagery on SVHS tape alleviates the problems of digital data storage but results in more data processing time and reduced temperature sensitivity and accuracy. In addition, imagery recorded on SVHS tape has a fixed 8-bit temperature range compared to digital imagery, which retains the full dynamic range of the thermal sensor.

Digital data collection also facilitates the process of correcting thermal imagery for atmospheric conditions because correction parameters can be applied to raw imagery postflight. Internally calibrated thermal imagers typically provide built-in methods to correct for atmospheric transmission with user-defined parameters of sensor–target distance, relative humidity, and ambient air temperature. It is necessary to correct for atmospheric conditions in thermal remote sensing of stream temperature because atmospheric transmission and absorption of longwave radiation by water vapor between the sensor and the stream surface influences remote measurements of water temperature. Temperature measurement error due to atmospheric conditions can be further reduced if thermal surveys are conducted from early to midafternoon when relative humidity is low and relatively constant. Additional error due to spatial variations in relative humidity can be reduced if atmospheric correction parameters are recorded during thermal overflights at remote automated weather stations throughout the survey area. Atmospheric radiation affects T_r and must be taken into account, but slight variations in atmospheric conditions (e.g., relative humidity differences between downstream and headwater reaches) have relatively little influence on T_r (Feijt & Kohsiek, 1995).

4.2. Thermal imagery of flowing waters

The physical variables that influence remote measurements of water temperature in rivers and streams are similar

to those encountered in remote observations of sea surface temperature from high-altitude and satellite platforms. Recent and extensive studies of TIR radiative properties of the ocean provide a basis for developing similar concepts in stream environments. Theoretical investigations into the factors that influence remote measurement of sea surface temperature have shown that the emissivity of the water surface varies with view angle, surface roughness (Masuda, Takashima, & Takayama, 1988; Sidran, 1981), turbidity, and salinity (Liu, Field, Gantt, & Klemas, 1987). Roughened water surfaces have lower emissivities and appear slightly warmer ($< 0.1^\circ$) than placid water surfaces of the same temperature (Masuda et al., 1988; Rees & James, 1992). Emissivity differences of 1% correspond to temperature differences of up to 0.5°C in satellite measurements of sea surface temperature (Feijt & Kohsiek, 1995). Effects of emissivity variation on T_r in natural stream surfaces have not been quantified, but evidence from marine environments suggests that thermal imagery of riffles, rapids, and pools contains information on surface roughness in addition to water temperature, particularly at low viewing angles. This means that slight variations in T_r (i.e., $< 0.5^\circ\text{C}$) may occur across smooth and rough water surfaces in a single thermal image even though T_k is constant.

4.2.1. Reflected and emitted TIR radiation

Interpretation of thermal imagery for water temperature assessment in rivers and streams requires an understanding of thermal radiative properties specific to the riverine environment (Fig. 1). Because the thermal sensor does not differentiate between reflected and emitted thermal radiation, temperatures in thermal imagery are a combination of both sources. Thus, it is necessary for the interpreter to determine visually which pixels most likely represent T_k . Thermal reflections from the sun are minimal in the 8–12 μm region, but reflections from clouds and surrounding terrestrial objects are visible in thermal imagery of stream surfaces, often in pronounced contrast with cold reflections from clear sky radiation (Svendsen, Jensen, Jensen, & Mogensen, 1990).

Reflection of thermal radiation from the sky and the surrounding terrestrial environment is dependent on view angle and water surface state. Reflectivity of thermal radiation on a smooth water surface in a controlled environment is low and constant at view angles $\leq 45^\circ$ from normal but increases dramatically at view angles $> 50^\circ$ (Wolfe & Zissis, 1985). On roughened water surfaces, reflectivity of thermal radiation increases considerably at view angles $\geq 25^\circ$ from normal (Sidran, 1981). Surface roughness determines whether thermal radiation is reflected specularly or diffusely. Specular reflections of cold sky radiation can be intense on smooth, mirror-like water surfaces. In contrast, diffuse reflections occur when radiation is scattered by multiple wave surfaces, thus creating the low intensity glitter of water bodies characteristic of reflections in the visible spectral region (Cox & Munk, 1954).

In thermal imagery of rivers and streams, pool surfaces were often observed to have a 0.4°C cooler temperature than adjacent riffles. The apparent difference was attributed to differences in reflective characteristics between pools and riffle surfaces in which cold sky reflections were scattered by the roughened water surface. We identified specular reflections in thermal imagery of stream surfaces by comparing thermal images with visible spectrum imagery in which surface roughness could be evaluated directly. As a consequence of the specular sky reflection effect, riffles provide more accurate sampling areas for T_r . Additionally, to minimize problems with reflections in thermal remote sensing of rivers and streams, particular care should be given to maintaining vertical view angles during aerial surveys.

4.2.2. Thermal boundary layer effects and stratification

Physical processes at the stream surface and turbulent mixing in the water column determine whether T_r is representative of T_k . Thermal stratification occurs at two different spatial scales: the micro level (mm) and the macro level (m) (Schluessel, Emery, Grassl, & Mammen, 1990). In the top few millimeters of the water surface, energy exchange between air and water results in evaporative heat loss from the top thin layer of the water surface and creates an aqueous thermal boundary layer 0.1–0.5°C cooler than underlying water (Robinson et al., 1984). The formation and persistence of the thermal boundary layer is dependent on heat flux, wind, and current stresses that disrupt the water surface.

A thermal imager is sensitive to water surface processes because the optical depth of the radiation detected is less than the thickness of the thermal boundary layer. This has proved useful in studies of energy flux and wave breaking in the ocean (Jessup et al., 1997). However, thermal boundary layer effects can also introduce average errors of 0.1–0.2°C in remote measurements of water temperature (Schluessel et al., 1990). In rivers and streams, thermal boundary layer effects are probably limited by streamflow in all but the most placid pool surfaces on which the thermal boundary layer has sufficient time to form. Research on temperature errors of this type in stream environments has not been conducted, but empirical work such as this is needed in order to further develop the application of TIR remote sensing in riverine environments.

Thermal stratification at the macro level can influence whether surface T_k is representative of T_k at depth. Below the thermal boundary layer, water is heated by shortwave radiation from the sun to a depth of 1 m (Schluessel et al., 1990). In the absence of turbulent mixing, water temperatures at depth are colder than surface temperatures, particularly when solar radiation reaches its peak in midafternoon. As a result, errors in water temperature measurement can occur in remote sensing of thermally stratified environments if the stratified condition is not recognized. Several factors determine whether the flow of water in a channel is

turbulent or laminar. The Reynolds number, Re , describes the relationship of these factors and is defined as

$$Re = \frac{\rho \nu r}{\mu}$$

where ρ is the fluid density (kg/m³), ν is the discharge velocity (m/s), r is the hydraulic radius (m) (the ratio of cross-sectional area to wetted perimeter in the stream channel), and μ is the water viscosity (kg/s m) (Fetter, 1994). The transition from laminar to turbulent flow occurs when Re exceeds a value of 2000. Simple calculations of Re provide a means to predict where remote temperature measurements may be influenced by thermal stratification. Where velocity data are unavailable for the calculation of Re , water velocity can be estimated using the Manning equation and stream gradient data from digital elevation models (Brooks, Ffolliot, Gregersen, & Thames, 1991).

Fluid dynamics theory suggests that turbulent flow is more common than laminar flow in rivers and streams (Narigasawa et al., 1988; Selby, 1985). Thus, thermal stratification is relatively uncommon in rivers and streams in which turbulent flow is sufficient to facilitate vertical mixing in the water column. In the reaches selected for studies of thermal stratification, field measurements of surface and bottom temperature verified Re predictions of turbulent flow at water velocities of 0.07–0.20 m/s. For the pool in GC4 with an average depth of 2 m, a minimum velocity of 0.0015 m/s would be required to cause turbulent flow and vertical mixing in the water column (Fig. 6A). Measurements of T_k (bottom–surface) do show minimal stratification in the deepest part of the pool (Fig. 6B). However, these measurements indicate that cool water from the bottom of the pool is being circulated, as predicted by Re , to the surface where it can be detected by remote sensing.

While laminar flow is uncommon in natural stream environments, thermal stratification can still occur if cold water enters the stream channel at a point where water velocity is very slow (Matthews, Berg, Azuma, & Lambert, 1994). Side channels and floodplain ponds with subsurface coldwater inputs present problems for remote measurement of stream temperature unless the springs can be detected as lateral inputs (Fig. 6C). Thermal remote sensing of stream environments requires at least some streamflow to provide accurate estimates of temperature in the water column. Thus, temperature measurements of isolated pools during low flow conditions will be strongly biased by warm surface water even though groundwater flow through the streambed may be cold. For these reasons, isolated groundwater inputs to the stream channel are best identified during winter months when groundwater is relatively warm and rises to the water surface.

4.3. Spatial and temporal analysis of stream temperature patterns

Airborne thermal remote sensing provides a method for assessing spatially continuous patterns of T_r in an entire

river over a short period of time. The spatiotemporal trade-off of high-resolution thermal imagery is that stream temperatures change over the course of an aerial survey. True synoptic surveys of stream temperature cannot be acquired using a low-altitude remote sensing platform because image data are collected sequentially in an upstream direction as opposed to areally in a single image. However, there are methods that minimize the spatiotemporal tradeoffs of longitudinal data collection. The upstream direction of the survey compensates for stream temperature change over the duration of the flight because rates of temperature change are generally slower in downstream reaches than in the headwaters (Vannote, Minshall, Cummins, Sedell, & Cushing, 1980). In addition, in-stream temperature recorders programmed to sample water temperature once every minute provide a temporally continuous context for temporally limited thermal imagery. During midafternoon surveys in July and August in eastern and western Oregon, water temperature changed at rates of 0–1°C/h within individual 50-km stream sections. By using in-stream temperature data, it is possible to correct spatially continuous thermal survey data for diurnal variations in stream temperature, but this requires assumptions to be made about temperature change in reaches without data recorders.

Stream temperatures change at different rates throughout a watershed depending on topography, riparian canopy structure, stream channel characteristics, water velocity, flow volume, and the relative influence of groundwater inputs (Brown, 1983). An advantage of thermal remote sensing is that it provides high-resolution information on spatial patterns of heating and cooling that result from these physical processes. Spatially continuous data on stream temperature patterns have only recently become available through technological improvements in thermal sensors and computerized geographic analysis. Thus, many questions remain about the actual causes of stream temperature patterns made visible for the first time through thermal remote sensing. Although thermal remote sensing of streams provides limited information on the hydrologic processes and mechanisms that influence stream temperature, it will be a highly effective tool for evaluating the patterns that emerge from these processes.

5. Conclusions

Airborne thermal remote sensing provides an effective means of mapping spatially continuous patterns of water temperature in rivers and streams. The concept of remote water temperature measurement has been applied successfully in ocean and lake environments using standard high-altitude platforms, but aerial methods for stream temperature assessment and analysis require a remote sensing system specifically designed for high-resolution, linear surveys of stream networks. Interpretation of water temperature data from thermal imagery requires an understanding of TIR

properties specific to the riverine environment because the radiative properties of flowing waters are influenced by multiple environmental factors and by the physical characteristics of the stream surface. In this article, we have presented a method for examining stream temperature at a resolution and extent previously unattainable through current methods of direct in-stream measurement; however, thermal imagery represents only one point in time and is most effective when used in conjunction with temperature data from in-stream monitoring stations. Spatially continuous temperature information from thermal remote sensing can be combined with temporally continuous data from in-stream temperature recorders and used to address current issues in water resources management and habitat conservation for aquatic organisms.

Acknowledgments

Funding for this project was provided by the U.S. Environmental Protection Agency (EPA), Advanced Monitoring Initiative; the EPA/National Science Foundation Joint Watershed Research Program (grant R82-4774-010 for ecological research); the Bonneville Power Administration (project No. 88-108 for salmon research); and the Confederated Tribes of the Warm Springs Reservation. Additional funding for thermal surveys of the McKenzie River was provided by the USDA Forest Service, McKenzie and Blue River Ranger Districts, the Central Cascades Adaptive Management Area, and the National Fish and Wildlife Foundation. Image collection services were provided by Snowy Butte Helicopters at Medford, OR. Data on groundwater processes in the Wenaha River were provided by C. Baxter and J. Ebersole in the Department of Fisheries and Wildlife, Oregon State University. Publication of this paper was supported, in past, by the Thomas G. Scott Achievement Grant.

References

- Anderson, J. M., Duck, R. W., & McManus, J. (1995). Thermal radiometry: a rapid means of determining surface water temperature variations in lakes and reservoirs. *Journal of Hydrology*, 173, 131–144.
- Anderson, J. M., & Wilson, S. B. (1984). The physical basis of current infrared remote-sensing techniques and the interpretation of data from aerial surveys. *International Journal of Remote Sensing*, 5, 1–18.
- Atwell, B. H., McDonald, R. B., & Bartolucci, L. A. (1971). Thermal mapping of streams from airborne radiometric scanning. *Water Resources Bulletin*, 7, 228–243.
- Avery, T. E., & Berlin, G. L. (1992). *Fundamentals of remote sensing and airphoto interpretation*. New York: Macmillan.
- Belknap, W., & Naiman, R. J. (1998). A GIS and TIR procedure to detect and map wall-base channels in western Washington. *Journal of Environmental Management*, 52, 147–160.
- Beschta, R. L. (1997). Riparian shade and stream temperature: an alternative perspective. *Rangelands*, 19, 25–28.

- Beschta, R. L., Bilby, R. E., Brown, G. W., Holtby, L. B., & Hofstra, T. D. (1987). Stream temperature and aquatic habitat: fisheries and forestry interactions. In: E. O. Salo, & T. W. Cundy (Eds.), *Streamside management: forestry and fishery interactions* (pp. 191–232). Seattle, WA: University of Washington, Institute of Forest Resources.
- Boyd, M., & Sturdevant, D. (1997). *The scientific basis for Oregon's stream temperature standard: common questions and straight answers*. Report, Oregon Department of Environmental Quality, Portland, OR.
- Brooks, K. N., Ffolliot, P. F., Gregersen, H. M., & Thames, J. L. (1991). *Hydrology and the management of watersheds*. Ames, IA: Iowa State Univ. Press.
- Brown, G. W. (1983). *Forestry and water quality*. Corvallis, OR: Oregon State University Bookstores.
- Chen, Y. D., Carsel, R. F., McCutcheon, S. C., & Nutter, W. L. (1998). Stream temperature simulation of forested riparian areas: 1. Watershed-scale model development. *Journal of Environmental Engineering*, *124*, 304–315.
- Chen, Y. D., McCutcheon, S. C., Norton, D. J., & Nutter, W. L. (1998). Stream temperature simulation of forested riparian areas: 2. Model application. *Journal of Environmental Engineering*, *124*, 316–328.
- Cox, C., & Munk, W. (1954). Measurement of the roughness of the sea surface from photographs of the sun's glitter. *Journal of the Optical Society of America*, *44*, 838–850.
- Davies, P. A., Mofor, L. A., & Neves, M. J. V. (1997). Comparisons of remotely sensed observations with modelling predictions for the behaviour of wastewater plumes from coastal discharges. *International Journal of Remote Sensing*, *18*, 1987–2019.
- Fagerlund, E. B., Kleman, B., Sellin, L., & Svensson, H. (1970). Physical studies of nature by thermal mapping. *Earth-Science Reviews*, *6*, 169–180.
- Feijt, A. J., & Kohsiek, W. (1995). The effect of emissivity variation on surface temperature determined by infrared radiometry. *Boundary-Layer Meteorology*, *72*, 323–327.
- Fetter, C. W. (1994). *Applied hydrogeology*. New York: Macmillan College Publishing.
- Frissell, C. A. (1992). *Cumulative effects of land use on salmon habitat in southwest Oregon coastal streams*. PhD thesis, Oregon State University, Corvallis, OR.
- Garrett, A. J., & Hayes, D. W. (1997). Cooling lake simulations compared to thermal imagery and dye tracers. *Journal of Hydraulic Engineering*, *123*, 885–894.
- Holtby, L. B. (1988). Effects of logging on stream temperatures in Carnation Creek, British Columbia, and associated impacts on the coho salmon (*Oncorhynchus kisutch*). *Canadian Journal of Fisheries and Aquatic Sciences*, *45*, 502–515.
- Jensen, J. R., Ramsey, E., Mackey, H. E. Jr., & Hodgson, M. E. (1988). Thermal modeling of heat dissipation in the Pen Branch Delta using thermal infrared imagery. *Geocarto International*, *3*, 17–28.
- Jessup, A. T., Zappa, C. J., Loewen, M. R., & Hesany, V. (1997). Infrared remote sensing of breaking waves. *Nature*, *385*, 52–55.
- Johnson, S. L., & Jones, J. A. (2000). Stream temperature responses to forest harvest and debris flows in western Cascades, Oregon. *Canadian Journal of Fisheries and Aquatic Sciences*, *57*, 30–39.
- Kneizys, F. X., Shettle, E. P., Gallery, W. O., Chetwynd, J. H., Abreu, L. W., Selby, J. E. A., Clough, S. A., & Fenn, R. W. (1988). Atmospheric transmittance/radiance: computer code LOW-TRAN-7. *AFGL-TR, 88-0177* (Air Force Geophysics Lab., Hanscomb AFB, Massachusetts).
- Larson, L. L., & Larson, S. E. (1996). Riparian shade and stream temperature: a perspective. *Rangelands*, *18*, 149–152.
- Lathrop, R. G. Jr., & Lillesand, T. M. (1987). Calibration of Thematic Mapper thermal data for water surface temperature mapping: case study on the Great Lakes. *Remote Sensing of Environment*, *22*, 297–307.
- LeBlanc, R. T., Brown, R. D., & FitzGibbon, J. E. (1997). Modeling the effects of land use change on the water temperature unregulated urban streams. *Journal of Environmental Management*, *49*, 445–469.
- LeDrew, E. F., & Franklin, S. E. (1985). The use of thermal infrared imagery in surface current analysis of a small lake. *Photogrammetric Engineering and Remote Sensing*, *51*, 565–573.
- Liu, W.-Y., Field, R. T., Gantt, R. G., & Klemas, A. (1987). Measurement of the surface emissivity of turbid waters. *Remote Sensing of the Environment*, *21*, 97–109.
- Masuda, K., Takashima, T., & Takayama, Y. (1988). Emissivity of pure and sea waters for the model sea surface in the infrared window regions. *Remote Sensing of the Environment*, *24*, 313–329.
- Matthews, K. R., Berg, N. H., Azuma, D. L., & Lambert, T. R. (1994). Cool water formation and trout habitat use in a deep pool in the Sierra Nevada, California. *Transactions of the American Fisheries Society*, *123*, 549–564.
- McCullough, D. A. (1997). *A review and synthesis of effects of alterations to the water temperature regime on freshwater life stages of salmonids, with special reference to chinook salmon*. Project Report, U.S. Environmental Protection Agency, Seattle, WA.
- Naiman, R. J., Magnuson, J. J., McKnight, D. M., Stanford, J. A., & Karr, J. R. (1995). Freshwater ecosystems and their management: a national initiative. *Science*, *270*, 584–585.
- Narigasawa, K., Gomi, Y., Komiyama, K., Fujisawa, K., Nakamura, I., & Kudo, M. (1988). Application of thermal infrared video system in spiral flow image tracing for the water flow velocity distribution measurement. *Geocarto International*, *2*, 51–56.
- Nehlsen, W., Williams, J. E., & Lichatowich, J. A. (1991). Pacific salmon at the crossroads: stocks at risk from California, Oregon, Idaho, and Washington. *Fisheries*, *16*, 4–21.
- Norton, D. J., Flood, M. A., McIntosh, B. A., Poage, N. J., LaPlaca, P. J., Craig, J. P., Karalus, R. S., Sedell, J. R., Torgersen, C. E., Chen, Y. D., McCutcheon, S. C., Duong, V., Puffenberger, H., Moeller, J., Kelly, V., Porter, E., & Shoemaker, L. (1996). *Modeling, monitoring and restoring water quality and habitat in Pacific Northwestern watersheds*. Project Report, U.S. Environmental Protection Agency, Washington, DC.
- NRC. (1992). *Restoration of aquatic ecosystems: science, technology, and public policy*. Washington, DC: National Research Council, National Academy Press.
- Poage, N. J., Torgersen, C. E., Norton, D. J., & Flood, M. A. (1996). Application of thermal infrared (FLIR) and visible videography to the monitoring and restoration of salmonid habitat in the Pacific Northwest. In: J. D. Greer (Ed.), *6th Forest Service Remote Sensing Applications Conference* (pp. 376–379). Denver, CO: American Society for Photogrammetry and Remote Sensing.
- Rees, W. G., & James, S. P. (1992). Angular variation of the infrared emissivity of ice and water surfaces. *International Journal of Remote Sensing*, *13*, 2873–2886.
- Ritchie, J. C., Grissinger, E. H., Murphey, J. B., & Garbrecht, J. D. (1994). Measuring channel and gully cross-sections with an airborne laser altimeter. *Hydrological Processes*, *8*, 237–243.
- Ritchie, J. C., Jackson, T. J., Garbrecht, J. D., Grissinger, E. H., Murphey, J. B., Everitt, J. H., Escobar, D. E., Davis, M. R., & Weltz, M. A. (1993). Studies using an airborne laser altimeter to measure landscape properties. *Hydrological Sciences*, *38*, 403–416.
- Robinson, I. S., Wells, N. C., & Charnock, H. (1984). The sea surface thermal boundary layer and its relevance to the measurement of sea surface temperature by airborne and spaceborne radiometers. *International Journal of Remote Sensing*, *5*, 19–45.
- Roxburgh, I. E. (1985). Thermal infrared detection of submarine springs associated with the Plymouth Limestone. *Hydrological Sciences*, *30*, 185–196.
- Schlüssel, P., Emery, W. J., Grassl, H., & Mammen, T. (1990). On the bulk-skin temperature difference and its impact on satellite remote sensing of sea surface temperature. *Journal of Geophysical Research*, *95*, 13341–13356.
- Schott, J. R. (1979). Temperature measurement of cooling water discharged from power plants. *Photogrammetric Engineering and Remote Sensing*, *45*, 753–761.
- Schott, J. R. (1994). Thermal infrared calibration of aerial and satellite

- images over land. In: *International Geoscience and Remote Sensing Symposium* (pp. 211–214). Pasadena, CA, USA: IEEE's Geoscience and Remote Sensing Society.
- Selby, M. F. (1985). *Earth's changing surface: an introduction to geomorphology*. Oxford, UK: Clarendon Press.
- Sidran, M. (1981). Broadband reflectance and emissivity of specular and rough water surfaces. *Applied Optics*, 20, 3176–3183.
- Smith, W. L., Knuteson, R. O., & Revercomb, H. E. (1996). Observations of the infrared radiative properties of the ocean: implications for the measurement of sea surface temperature via satellite remote sensing. *Bulletin of the American Meteorological Society*, 77, 41–51.
- Svendsen, H., Jensen, H. E., Jensen, S. E., & Mogensen, V. O. (1990). The effect of clear sky radiation on crop surface temperature determined by thermal thermometry. *Agricultural and Forest Meteorology*, 50, 239–243.
- Torgersen, C. E., Price, D. M., Li, H. W., & McIntosh, B. A. (1999). Multiscale thermal refugia and stream habitat associations of chinook salmon in northeastern Oregon. *Ecological Applications*, 9, 301–319.
- Vannote, R. L., Minshall, G. W., Cummins, K. W., Sedell, J. R., & Cushing, C. E. (1980). The river continuum concept. *Canadian Journal of Fisheries and Aquatic Sciences*, 37, 130–137.
- Wolfe, W. L., & Zissis, G. J. (1985). *The infrared handbook*. Washington, DC: Office of Naval Research.
- Zwieniecki, M. A., & Newton, M. (1999). Influence of streamside cover and stream features on temperature trends in forested streams of Western Oregon. *Western Journal of Applied Forestry*, 14, 106–113.